INSTITUTE

for

FLUID DYNAMICS

and

APPLIED MATHEMATICS

Tech. Note BN-721 January 1972

DETERMINATION OF SOUNDING ROCKET POSITION AND ATTITUDE FROM RADAR AND MAGNETOMETER DATA

Morris Pongratz
University of Maryland
College Park, Maryland
20742

UNIVERSITY OF MARYLAND
College Park

DETERMINATION OF SOUNDING ROCKET POSITION AND ATTITUDE FROM RADAR AND MAGNETOMETER DATA*

by

Morris Pongratz
University of Maryland
College Park, Maryland
20742

*This work was supported by the National Aeronautics and Space Administration under research grant NSR 21-002-077. Machine computation was performed by the Computer Science Center of the University of Maryland and was supported by NASA grant ~~NSG-398~~ NGL-21-002-008.

ABSTRACT

This report describes the techniques used to determine the trajectories and orientations of three sounding rockets instrumented to study the aurora. The radar plot board data were fitted to a near earth expansion of the force of gravity to determine the trajectory. Only onboard magnetometer data were used to determine the attitude of the payload with respect to the earth's magnetic field. Computer programs in the FORTRAN language are available which generate the trajectory and attitude parameters.

Chapter I

Introduction

We have launched three Nike-Tomahawk sounding rockets* from Fort Churchill, Canada, to study aurorae. In order to determine pitch angle information about energetic electrons and for analysis of data from other experiments on board it is necessary to be able to describe the position and attitude of the payload. The payloads are launched with a Nike booster which falls away when spent and a Tomahawk second stage which burns out before atmospheric exit and remains attached to the payload. Flight duration and apogee are typically 500 seconds and 250 km respectively. To achieve stability the vehicles are spun at about 7 rps during burning. After burn-out they are despun to about 1 rps to facilitate collection of angular information in the data. Radar plots furnished by the Churchill Research Range were used to determine vehicle position. On board magnetometers which measured the component of the earth's magnetic field parallel to their orientation were used to determine payload attitude.

Chapter II

Vehicle Position

The effects of coriolis and centripetal accelerations upon sounding rockets launched from Churchill show up most dramatically in reducing the eastward distance traveled by several kilometers (the earth rotates under the payload). The North-South location of the impact point is virtually unaffected. In practice one is most concerned with the effect upon the

*NASA 18.63 UE, 18.64 UE and 18.65 UE.

altitude where the effect of centripetal acceleration is less than 0.1%. However, since most vehicles are launched eastward the coriolis acceleration is in the opposite sense to the centripetal acceleration and can be of nearly the same magnitude so one can safely ignore these effects. Because the exact impact point is generally not needed and because radar data frequently is not good enough to justify further precision we will adopt a coordinate system assuming a flat, nonrotating earth with positive z representing attitude and positive x representing eastward direction. Normally a flat earth assumption would have g, the acceleration of gravity, independent of z. However over the range of z for the sounding rocket this represents an appreciable error so we will use an expansion of the potential energy, V, for the inverse square gravitational force,

$$V = -\frac{GM_e m}{r} = \frac{-GM_e m}{R_e+z} \tag{2-1}$$

where G is the gravitational constant, M_e is the mass of the earth, m is the mass of the payload, r is radial distance from center of the earth and R_e is the radius of the earth at Churchill.

Expanding (2-1) in z/R_e gives

$$\begin{aligned} V &= \frac{-GM_e m}{R_e}\,(1+z/R_e)^{-1} \\ &= \frac{-GM_e m}{R_e}\,[1-z/R_e + (z/R_e)^2 - (z/R_e)^3 + \ldots] \\ &= \frac{-GM_e m}{R_e} + \frac{GM_e m}{R_e^2}\,z - \frac{GM_e m}{R_e^3}\,z^2 \end{aligned}$$

neglecting the cubic and higher terms.

The payload kinetic energy can be written,

$$T = 1/2\ m\ (\dot{x}^2 + \dot{y}^2 + \dot{z}^2) \quad . \tag{2-3}$$

Hence the Lagrangian is,

$$L = T - V = 1/2\ m\ (\dot{x}^2 + \dot{y}^2 + \dot{z}^2) + \frac{GM_e m}{R_e} - \frac{GM_e m}{R_e^2}\ z + \frac{GM_e m}{R_e^3}\ z^2 \quad . \tag{2.4}$$

Since x and y do not appear in L the corresponding velocities are constant above the atmosphere. The differential equation in z is

$$\ddot{z} = -\frac{GM_e}{R_e^2} + 2\frac{GM_e}{R_e^2}\ \frac{z}{R_e} = -g_o + 2\ g_o\ \frac{z}{R_e} \tag{2-5}$$

where g_o is the acceleration of gravity on surface pf earth,

$$g_o \equiv \frac{GM_e}{R_e^2} \quad . \tag{2-6}$$

The general solution to (2-5) is

$$z = B_1\ e^{\alpha t} + B_2 e^{-\alpha t} + B_3 \tag{2-7}$$

where α and B_3 are given by,

$$\alpha = (2g_o/R_e)^{1/2} \qquad B_3 = R_e/2 \quad . \tag{2-8}$$

Using (2-6) and the value of g measured at Churchill of $g = 981.761\ cm/sec^2$ one can solve for the value of R_e to use. These values are in Table I.

Table I

$R_E = 6377.0$ km

$B_3 = 3188.5$ km

$\alpha^2 = 0.307907 \times 10^{-5}$ sec^{-2}

$\alpha = 0.175473 \times 10^{-2}$ sec^{-1}

The problem remaining is to use the measured z_i and t_i from the radar plot to least squares fit for the initial conditions B_1 and B_2. This analysis was quite satisfactory for 18:63 and 18:64, but for 18:65 we obtained a better fit to the points using slightly different values for R_E and fitting for B_3 also.

Apogee time, t_A, and height, z_A, can be found by differentiating (2-7)

$$t_A = \frac{1}{2} \ln (B_2/B_1)^{1/2} \tag{2-9}$$

$$z_A = -2 (B_1 B_2)^{1/2} + B_3 . \tag{2-10}$$

The values for liftoff time, t_A, z_A and the four coefficients in (2-7) for t and t_A measured from liftoff are given in Table II.

Table II

Vehicle	Liftoff	t_A	z_A[km]	B_1[km]	B_2[km]	B_3[km]	α[sec^{-1}]
18:63	21 Mar '68 0601:32.7	241.09	241.76	-965.129	-2249.25	3188.5	0.17547×10^{-2}
18:64	14 Jan '70 0405:30.0	250.24	259.74	-943.961	-2271.7	3188.5	0.17547×10^{-2}
18:65	17 Jan '70 0303:20.0	248.16	252.48	-779.05	-1989.9	2742.7	0.18894×10^{-2}

One can use (2-7) to determine v_z by differentiation. Figures 1 - 3 are plots of the altitude and v_z versus Universal Time in minutes. The x and y components of velocity are given in Table III.

Table III

Vehicle	v_x (East) [km/sec]	v_y (North) [km/sec]	v_{xy} [km/sec]
18:63	0.051	- 0.101	0.113
18:64	0.203	- 0.005	0.206
18:65	0.276	0.168	0.322

It is interesting to compare the altitude at which the payloads were inverted by the atmospheric drag on the fins and the altitude at which the electronics began experiencing sustained high voltage breakdowns in Table IV.

Table IV

Vehicle	Turnover altitude [km]	Breakdown altitude [km]
18:63	72	83
18:64	65	81
18:65	73	81

Because the radar did not track the payloads throughout the flights there may be several kilometer uncertainties in z below about 120 km on the downward leg of the flight. The uncertainty on the upward leg is on the order of 100 meters. It is possible to obtain an exact analytical solution to this problem for t as a function of z , but it would be very difficult to use least squares technique to obtain the initial conditions.

Chapter III

Payload Attitude

After despin the payload is sufficiently above the atmosphere to enable one to neglect torques due to atmospheric friction. In the absence of net torques $\vec{L}$, the total angular momentum vector, is constant in an inertial frame. We will then choose the direction of $\vec{L}$ to be the $+ z'$ direction of the space axes for our description of payload attitude. This space set of axes is not the system used to describe position of the payload. More aspect information than supplied by the magnetometers is necessary to relate the two systems.

Barring the unfortunate and rare case where $\vec{L}$ and $\vec{B}$ would be parallel or antiparallel we will use the direction of $\vec{B}$ to provide the other direction necessary for the space axes. Assuming that over the altitude and temporal range of interest $\vec{B}$ is nearly constant in direction we define the x' direction by specifying that $\vec{B}$ lie in the $x' - z'$ plane and that $B_{x'}$, the component of $\vec{B}$ parallel to x', be negative. In a simplified case where $\vec{L}$ is in the local vertical direction and the magnetic declination is zero this coordinate system would have the x' axis pointing south (equatorward from Churchill) and the y' axis pointing eastward because the magnetic field is in the northward direction. Figure 4 represents this simplified case. In this coordinate system we can describe the magnetic field as

$$(3\text{-}1) \qquad \vec{B} = B_o(t)\,\hat{b} = B_{x'}(t)\,\hat{i}' + B_{z'}(t)\,\hat{k}' = B_o(t)\,[\sin\beta\,\hat{i}' + \cos\beta\,\hat{k}']$$

where the magnitude of $\vec{B}$, $B_o(t)$, does have the altitude dependence, through t, and β is the angle between $\vec{B}$ and $\hat{k}'$, the unit vector along $\vec{L}$.

By definition of $\hat{i}'$ $\cos\beta < 0$ and for a typical $\vec{L}$ direction $\sin\beta < 0$ so β would lie in the third quadrant.

The body coordinate system, x'' y'' z'', is used to describe position and orientation within the payload. We choose the z'' axis to be a principal axis and assume that it coincides with the symmetry axis whcih describes the axial dimension of the payload parallel to the geometric center line and in the direction of the nose of the payload. The x'' and y'' axes are also principal axes and are assumed along the directions specified by the magnetometers as in Figure 5. The origins of the two systems coincide at the center of gravity of the payload.

For time-independent moments of inertia (the slowly despinning case will be considered in an appendix) and for a rigid body rotating about its center of gravity with body-fixed axes coinciding with the principal axes Eulers equations are

$$
\begin{aligned}
I_{x''x''}\,\dot{\omega}_{x''} &= \omega_{y''}\omega_{y''}\,(I_{y''y''} - I_{z''z''}) \\
I_{y''y''}\,\dot{\omega}_{y''} &= \omega_{z''}\omega_{x''}\,(I_{z''z''} - I_{z''x''}) \\
I_{z''z''}\,\dot{\omega}_{z''} &= \omega_{x''}\omega_{y''}\,(I_{x''x''} - I_{y''y''}) \quad .
\end{aligned}
\tag{3-2}
$$

Because of the symmetry about the z'' axis we can define transverse, I_T, and axial, I_A, moments of inertia

$$
\begin{aligned}
I_{x''x''} &= I_{y''y''} \equiv I_T \\
I_{z''z''} &\equiv I_A \quad .
\end{aligned}
\tag{3-3}
$$

For our payloads $I_T >> I_A$ ($I_T \sim 200\ I_A$) . Equations (3-2) now can be written

$$
\begin{aligned}
I_T\,\dot{\omega}_{x''} &= \omega_{y''}\omega_{z''}\,(I_T - I_A) \\
I_T\,\dot{\omega}_{y''} &= -\,\omega_{z''}\omega_{x''}\,(I_T - I_A) \\
I_A\,\dot{\omega}_{z''} &= 0 \quad .
\end{aligned}
\tag{3-4}
$$

From the last of equations (3-4) we have

$$
\dot{\omega}_{z''} = 0 \quad ; \quad \omega_{z''} = \text{constant} \ . \tag{3-5}
$$

Define $\Omega \equiv \omega_{z''}\left(\frac{I_T - I_A}{I_T}\right)$, then equations (3-4) become

$$
\begin{aligned}
\dot{\omega}_{x''} &= \omega_{y''}\Omega \\
\dot{\omega}_{y''} &= \omega_{x''}\Omega \\
I_A\,\dot{\omega}_{z''} &= 0 \ .
\end{aligned}
\tag{3-6}
$$

The first two equations can be combined to give

$$
\begin{aligned}
\dot{\omega}_{x''} - \omega_{y''}\Omega &= 0 \\
\dot{\omega}_{y''} + \omega_{x''}\Omega &= 0 \ .
\end{aligned}
\tag{3-7}
$$

Multiplying the first equation by $\omega_{x''}$ and the second by $\omega_{y''}$ and summing them gives

$$
\dot{\omega}_{x''}\omega_{x''} + \dot{\omega}_{y''}\omega_{y''} = 0 \ . \tag{3-8}
$$

Equation (3-8) can be integrated to give

$$
\omega_{x''}^2 + \omega_{y''}^2 = \text{constant} \equiv \omega_T^2 \tag{3-9}
$$

therefore from (3-5) and (3-9) we have,

(3-10) $$|\vec{\omega}| = \sqrt{\omega_{x''}^2 + \omega_{y''}^2 + \omega_{z''}^2} = \sqrt{\omega_{z''}^2 + \omega_T^2} = \text{constant},$$

the angular velocity vector has constant magnitude.

Assuming constant Ω one can differentiate the first of equations (3-6) and substitute in the second one to give

(3-11) $$\ddot{\omega}_{x''} = \dot{\omega}_{y''}\Omega = -\omega_{x''}\Omega^2 .$$

Equation (3-11) describes simple harmonic motion for $\omega_{x''}$. For typical initial conditions let $\omega_{x''} = 0$ and $\omega_{y''} = \omega_T$ using (3-9). Then we can write for $\omega_{x''}$ and $\omega_{y''}$

(3-12) $$\omega_{x''} = \omega_T \sin \Omega t$$
$$\omega_{y''} = \omega_T \cos \Omega t .$$

We can also write $\vec{\omega}$ and $\vec{L}$ in the body frame

(3-13) $$\vec{\omega} = \omega_{x''}\,\hat{i}'' + \omega_{y''}\,\hat{j}'' + \omega_{z''}\,\hat{k}''$$
$$= \omega_T (\sin \Omega t\, \hat{i}'' + \cos \Omega t\, \hat{j}'') + \omega_{z''}\hat{k}''$$
$$\vec{L} = \overleftrightarrow{I}\cdot\vec{\omega}$$
$$= I_T \omega_T (\sin \Omega t\, \hat{i}'' + \cos \Omega t\, \hat{j}'') + I_A \omega_{z''}\, \hat{k}'' .$$

From Figure 6 we can obtain the angle θ between $\vec{L}$ and the z" axis, and ε, the angle between $\vec{\omega}$ and the z" axis.

(3-14) $$\tan \theta = \frac{I_T \omega_T}{I_A \omega_{z''}}$$

(3-15) $$\tan \varepsilon = \frac{\omega_T}{\omega_{z''}} .$$

Since $I_T > I_A$, $\vec{\omega}$ lies between $\vec{L}$ and the z" axis. The angles θ and ε are constant because the quantities on the right hand side of equations (3-14) and (3-15) are constant.

$$\dot{\theta} = \dot{\varepsilon} = 0 \qquad \theta = \theta_o \quad , \quad \varepsilon = \varepsilon_o \quad . \tag{3-16}$$

We use the Euler angles to refer the body system to the space fixed system. Note that the angle θ is also the Euler angle θ (see Figure 7). The transformation between the two sets of axes is given by[1]

$$\begin{aligned} \omega_{x''} &= \dot{\phi} \sin\theta \sin\psi + \dot{\theta} \cos\psi \\ \omega_{y''} &= \dot{\phi} \sin\theta \cos\psi - \dot{\theta} \sin\psi \\ \omega_{z''} &= \dot{\phi} \cos\theta + \dot{\psi} \end{aligned} \tag{3-17}$$

Using (3-16) these equations become

$$\begin{aligned} \omega_{x''} &= \dot{\phi} \sin\theta \sin\psi \\ \omega_{y''} &= \dot{\phi} \sin\theta \cos\psi \\ \omega_{z''} &= \dot{\phi} \cos\theta + \dot{\psi} \quad . \end{aligned} \tag{3-18}$$

From (3-9) and (3-18) we have

$$\omega_{x''}^2 + \omega_{y''}^2 = \omega_T^2 = \dot{\phi}^2 \sin^2\theta \; . \tag{3-19}$$

Using (3-16) and (3-19) we can define the precession frequency, ω_p , by

$$\dot{\phi} = \text{constant} \equiv \omega_p \; . \tag{3-20}$$

From the last of equations (3-18) and (3-5) and (3-20) we can define the spin frequency, ω_s ,

(3-21) $$\dot{\psi} = \text{constant} \equiv \omega_s \ .$$

Differentiating (3-18) and substituting them into the first equation of (3-4) gives

(3-22) $$I_T \dot{\phi}\dot{\psi} \sin\theta \cos\psi = (\dot{\phi} \sin\theta \cos\psi)\ (\dot{\phi} \cos\theta + \dot{\psi})\ (I_T - I_A)$$

which can be solved for $\dot{\phi}$ in terms of $\dot{\psi}$

(3-23) $$\omega_p = \dot{\phi} = \frac{I_A \dot{\psi}}{(I_T - I_A) \cos\theta} = \frac{\omega_s}{\cos\theta} \frac{1}{\left(\frac{I_T}{I_A} - 1\right)}$$

and we have the ratio of spin frequency to precession frequency

(3-24) $$\omega_s/\omega_p = \left(\frac{I_T}{I_A} - 1\right) \cos\theta \ .$$

Using (3-16), (3-20) and (3-21) we can write the Euler angles in terms of their time derivatives

(3-25) $$\begin{aligned} \theta &= \theta_o \\ \phi &= \omega_p t + \phi_o \\ \psi &= \omega_s t + \psi_o \ . \end{aligned}$$

We are now prepared to describe the way the magnetic field, $\vec{B}$, which is fixed in the space frame will be seen by the magnetometers on board the payload - the body frame.

The magnetometers measure the component of magnetic field parallel to their orientation. They output a bias voltage, CB, of about 2.5 V plus a voltage linearly dependent upon the magnitude of the component of $\vec{B}$ parallel to their orientation. The linear coefficient, CA, is

about 4.0V/Gauss. Let $\hat{n}_i''$ be a unit vector in body frame in the direction measured by the i magnetometer, then the output voltage, V_i, has the form

$$V_i = CA_i \vec{B} \cdot \hat{n}_i'' + CB_i \quad . \tag{3-26}$$

Therefore if $\vec{B}$ is antiparallel to $\hat{n}_i''$ the output is less than CB_i and vice-versa. The analysis used here will assume the form of (3-26) for V_i and neglect non-linear terms.

From (3-26), if $\vec{B}$ and $\hat{n}_i''$ were measured in the same frame, the output voltage would be a constant term modulated by a cosine term, but alas all is not so simple! We need to know the components of $\vec{B}$ in the body frame to be able to compute the dot product required in (3-26). This transformation, using (3-1), is given by

$$\vec{B}'' = \overleftrightarrow{A} \cdot \vec{B} = B_o(t) \overleftrightarrow{A} \begin{pmatrix} \sin\beta \\ o \\ \cos\beta \end{pmatrix} \tag{3-27}$$

where $\overleftrightarrow{A}$ is[2]

$$\overleftrightarrow{A} = \begin{pmatrix} \cos\psi\cos\phi - \cos\theta\sin\phi\sin\psi & \cos\psi\sin\phi + \cos\theta\cos\phi\sin\psi & \sin\psi\sin\theta \\ -\sin\psi\cos\phi - \cos\theta\sin\phi\cos\psi & -\sin\psi\sin\phi + \cos\theta\cos\phi\cos\psi & \cos\psi\sin\theta \\ \sin\theta\sin\phi & -\sin\theta\cos\phi & \cos\theta \end{pmatrix} . \tag{3-28}$$

Equation (3-27) then becomes

$$\vec{B}'' = \overleftrightarrow{A} \cdot \vec{B} = B_{x''}\,\hat{i}'' + B_{y''}\,\hat{j}'' + B_{z''}\,\hat{k}'' \tag{3-29}$$

where

$$B_{x''} = B_o(t)\,[\sin\beta\,(\cos\psi\cos\phi - \cos\theta\sin\phi\sin\psi) + \cos\beta\sin\psi\sin\theta]$$

$$B_{y''} = B_o(t)\,[\sin\beta\,(-\sin\psi\cos\phi - \cos\theta\sin\phi\cos\psi) + \cos\beta\cos\psi\sin\theta] \tag{3-30}$$

$$B_{z''} = B_o(t)\,[\sin\beta\sin\theta\sin\phi + \cos\beta\cos\theta]\ .$$

Now one can compute the dot products for the three possible magnetometers measuring the x'', y'', z'' components of the field. For the x'' component, $\hat{n}_{i''}$ in (3-26), is $\hat{i}''$ and

$$\vec{B}'' \cdot \hat{n}_{x''} = B_o(t)\,[\sin\beta\cos\psi\cos\phi - \sin\beta\cos\theta\sin\phi\sin\psi + \cos\beta\sin\psi\sin\theta]\ . \tag{3-31}$$

For the y'' component, $\hat{n}_{i''}$ is $\hat{j}''$ and

$$\vec{B}'' \cdot \hat{n}_{y''} = B_o(t)\,[-\sin\beta\sin\psi\cos\phi - \sin\beta\cos\theta\sin\phi\cos\psi + \cos\beta\cos\psi\sin\theta]\ . \tag{3-32}$$

For the z'' component $\hat{n}_{i''}$ is $\hat{k}''$ and

$$\vec{B}'' \cdot \hat{n}_{z''} = B_o(t)\,[\sin\beta\sin\theta\sin\phi + \cos\beta\cos\theta]\ . \tag{3-33}$$

To simplify these equations we define

$$\begin{aligned} a &= \sin\beta\sin\theta \\ b &= \cos\beta\cos\theta \\ c &= \sin\beta\cos\theta \\ d &= \cos\beta\sin\theta \\ e &= d - c\sin\phi \\ f &= \sin\beta\cos\phi\ . \end{aligned} \tag{3-34}$$

We shall restrict ourselves to the case where $\vec{L}$ is upward rather than downward over Churchill.This is the condition before despin and it is improbable that despinning could invert the payload angular momentum vector. For 18:64 and 18:65 the z" axis magnetometers indicate that $\vec{L}$ remained nearly vertical. This assumption puts β in the third quadrant and makes the first four quantities defined in (3-34) negative.

The resulting equations are

$$\vec{B}'' \cdot \hat{n}_{x''} = B_o(t)\,[e \sin\psi + f \cos\psi] \tag{3-35}$$

$$\vec{B}'' \cdot \hat{n}_{y''} = B_o(t)\,[e \cos\psi - f \sin\psi] \tag{3-36}$$

$$\vec{B}'' \cdot \hat{n}_{z''} = B_o(t)\,[a \sin\phi + b]\ . \tag{3-37}$$

We choose t in equation (3-25) to be zero at a time when the payload (and z'' axis) is most antiparallel to $\vec{B}$ (when z'' is nearest $-\vec{B}$). This means that equation (3-37) is at a minimum value indicating $(a < 0)$ that $\sin\phi$ is unity, hence

$$\begin{aligned} \phi(t = 0) \equiv \phi_o &= \pi/2 \\ e_o \equiv e(t = 0) &= d - c \\ f_o \equiv f(t = 0) &= 0\ . \end{aligned} \tag{3-38}$$

Because ϕ varies much slower than ψ one can also require that $t = 0$ be chosen at a time where $V_{y''}$, the voltage from y'' - axis magnetometer (the RAM-) is less than $CB_{y''}$ - the bias value. This means that (3-36) is at a minimum value at $t = 0$. Recalling that $f_o = 0$ determines ψ_o to be 0 or π depending upon the sign of e_o. Because c and d are typically both negative we can define a positive quantity, g,

$$g \equiv c/d = \tan\beta/\tan\theta\ . \tag{3-39}$$

If $g > 1$, then $e_o > 0$ and $\psi_o = \pi$ and if $g < 1$, $e_o < 0$ and $\psi_o = 0$. Since β is in the third quadrant (3-39) implies that if $\beta - \pi > \theta$, $\psi_o = \pi$ whereas if $\beta - \pi < \theta$, $\psi_o = 0$. When $\beta - \pi > \theta$ the payload precession cone does not include $\vec{B}$ and when $\beta - \pi < \theta$ the precession cone does include $\vec{B}$. Hence, if the payload precesses around $\vec{B}$, $\psi_o = 0$ and if the payload does not precess around $\vec{B}$, $\psi_o = \pi$. Figures 8 and 9 show the two cases.

We will now outline the procedure for determining the two constant angles θ and β. We have measured the times and voltages at local maxima and minima on the y" - axis magnetometer and x" - axis magnetometer for 18:64 and 18:65 respectively. 18:63 had only the y" - axis magnetometer. For 18:64 and 18:65 we made detailed, simultaneous measurements from all three magnetometers during the several second time interval where the payloads turned over and all three magnetometers sampled a full range of values. Taking advantage of the fact that the magnitude of the field was nearly constant over this short time interval we were able to make self-consistent checks on the calibrated values of the CA's and CB's.

We also picked several times encompassing the complete altitude range where we simultaneously measured the voltage output from all three magnetometers. Using the calibrations we converted these voltages into values for the magnetic field components parallel to the three axes. We then summed the components to obtain the field magnitudes.

$$B_o(t) = [B_{x''}{}^2(t) + B_{y''}{}^2(t) + B_{z''}{}^2(t)]^{1/2} \quad , \tag{3-40}$$

over a range of altitudes. We found that we could model the altitude dependence as

$$B_o(t) = B_o(z(t)) = \frac{B_{oo}}{(R_E+z(t))^3} \tag{3-41}$$

as would be expected for a dipole field model.

The next step is to look at the components of $\vec{B}$ which are parallel and perpendicular to the payload spin axis, z" . Let α be the instantaneous angle between the z" axis and $\vec{B}$, then we define

$$B_{\perp} \equiv |\vec{B}| \sin \alpha$$

(3-42)

$$B_{||} \equiv |\vec{B}| \cos \alpha$$

$$|\vec{B}| \equiv (B_{\perp}^2 + B_{||}^2)^{1/2} = B_o(t) .$$

Since we measure x" or y" magnetometer voltages only at their local maxima or minima the corresponding y" or x" magnetometers are perpendicular to $B_{\perp}$ and measure no field at these times. Hence, by measuring the voltages at local maxima and minima we know that they correspond to the instantaneous value of $B_{\perp}$. The import of this is that in general the dot product in (3-26) for the x" magnetometer is

$$\vec{B} \cdot \hat{n}_{x"} = B_{x"}$$

which is only some part of $B_{\perp}$, but at the special times we measured $V_{x"}$ we have $B \cdot n_{x"} = B_{x"} = B_{\perp} = B_o(t) \sin \alpha$.

To generalize let m refer to the indices x" or y" when y" or x" respectively are perpendicular to the field, then (3-26) becomes

(3-43) $$V_m = CA_m B_o(t) \sin \alpha + CB_m .$$

Equation (3-43) has only $\sin \alpha$ unknown. It can be solved for $\sin \alpha$ and then for $\cos \alpha$,

(3-44) $$\cos \alpha = \pm \left[1 - \frac{(V_m - CB_m)^2}{(CA_m B_o(t))^2} \right]^{1/2} .$$

We will choose the negative sign in (3-44) when we can tell from the envelope of the values of V_m that the z" axis is still above the magnetic horizon. This will be discussed in further detail later.

Of course, cos α is very easy to compute from the output of the z" - axis magnetometer,

(3-45)
$$V_{z"} = CA_{z"}\, B_o(t) \cos\alpha + CB_{z"}$$
$$\cos\alpha = \frac{V_{z"} - CB_{z"}}{CA_{z"}\, B_o(t)}$$

here there is no ambiguity about the sign of cos α .

Comparison of (3-26) , (3-37) and (3-45) shows that

(3-46)
$$\cos\alpha = b + a \sin\phi \ .$$

By inspection of the envelope curve for a node or by finding minima in $B_\perp$ one can determine the Universal Time , t_o , where the z" axis is closest to $-\vec{B}$ and the voltage is a local minimum. The time to the next similar node gives τ_p , the precession period. One can then write ϕ

(3-47)
$$\phi = \left(\frac{2\pi}{\tau_p}\right) t + \phi_o$$

where $t = t^* - t_o$ and $\phi_o = \pi/2$ and t^* is Universal Time.

Armed with an expression for ϕ one can perform a least squares fit to equation (3-46) to determine the constants a and b . Using the first two equations of (3-34) we found two pairs of β and θ ($a < 0$, $b < 0$) . One pair, β_1 and θ_1 , corresponds to a precession cone not including $\vec{B}$ and the other pair, β_2 and θ_2, does correspond to z" - axis precession around $\vec{B}$.

Vehicle 18:63 had only a y" - axis magnetometer which was shifted upwards in $CB_{y''}$ and consequently for much of the flight local maxima of $V_{y''}$ were greater than the telemetry voltage limit. We also suffered some telemetry dropouts which unfortunately coincided in time with the local maxima and minima of $V_{y''}$ further hampering data reduction. To fill the gaps where $V_{y''}$ could not be measured at local minima or maxima we decided to use the values of local maxima or minima of $V_{y''}$ which were reconstructed from the slope of $V_{y''}$ evaluated at $CB_{y''}$. We had about 90 directly measured values and about 50 indirectly measured values of $V_{y''}$ with some overlapping to check the accuracy of the slope reconstruction method.

Using (3-26) and (3-36) we have

$$V_{y''} = CA_{y''} B_o(t) [e \cos \psi - f \sin \psi] + CB_{y''} . \tag{3-48}$$

The expression in brackets can be written

$$[e \cos \psi - f \sin \psi] = h \sin (\psi_o - \psi) \tag{3-49}$$

where $h^2 = e^2 + f^2$ and $\tan \psi_o = e/f$. Taking advantage of the fact that $B_o(t)$, e and f are nearly constant over a few spin periods one can compute the derivative of (3-48),

$$\begin{aligned} \frac{\partial V_{y''}}{\partial t} &= CA_{y''} B_o(t) h \cos (\psi_o - \psi) (-\dot{\psi}) \\ &= - CA_{y''} B_o(t) h \dot{\psi} \cos (\psi_o - \psi) . \end{aligned} \tag{3-50}$$

But we measured the slope where $V_{y''} = CB_{y''}$ which meant that $\psi_o - \psi = n\pi$ and consequently $\cos (\psi_o - \psi) = \pm 1$. This means that we can solve (3-50)

for h in terms of known quantities ($\dot{\psi}$ is the spin frequency which for 18:63 could be directly measured to a few percent),

$$(3\text{-}51) \qquad h = \mp \left(\frac{\partial V_{y''}}{\partial t} \right)_{V_{y''} = CB_{y''}} / CA_{y''} B_o(t) \dot{\psi} \quad .$$

But at a time $\pm \tau_s/4$ from where $V_{y''} = CB_{y''}$ the angle ψ will change to where $\sin(\psi_o - \psi) = \pm 1$ and we can substitute the value of h from (3-51) into (3-49) - (3-48) to get

$$(3\text{-}52) \qquad V_{y''} = \mp \left(\frac{\partial V_{y''}}{\partial t} \right)_{V_{y''} = CB_{y''}} / \dot{\psi} + CB_{y''} \quad .$$

Therefore by measuring the slope and spin rate we were able to reconstruct values to give the correct envelope voltages to use in determining θ and β. This method was checked in several overlap regions by measuring both the slope and local maxima and minima and the results agreed to within 4 %.

Normally the envelope of local maxima-minima voltages will exhibit nodes with the frequency of the precession of z'' about $\vec{L}$. These nodes correspond to times where the z'' - axis is nearest to $-\vec{B}$. For 18:63 secondary nodes betweeen precession period nodes indicated that the z'' - axis had dropped below the magnetic horizon giving the envelope primary nodes when $\phi = \pi/2 + 2n\pi$ and secondary nodes when $\phi = 3\pi/2 + 2n\pi$ (see figure 10). This was very fortunate giving a built-in calibration of the product $CA_m B_o(t)$ in equation (3-44) at the times when the payload was perpendicular to $\vec{B}$. Equation (3-46) had /a/>/b/ and we varied the amount of time spent below the magnetic horizon to give the best fit to the measured envelope. Figure 11 indicates that the fit was very good except when α was near 90° when the telemetry problem was most severe.

By measuring times of adjacent magnetometer maxima and minima one can determine the spin frequency, ω_s to only about ± 4% because (3-48) for example is not a pure sine wave and the time between adjacent maxima reflects variations in parameters other than ψ alone. To improve this measurement we counted the number of oscillations, n_o, in an approximate precession period (to the nearest complete cycle). We then accurately (± 5 ms) measured the time elapse, Δt, during the n_o oscillations. The hypothesis was then made that ω_s had one of the three values given by

$$\omega_{s_-} = \frac{2\pi(n_o-1)}{\Delta t}$$

$$\omega_{s_o} = \frac{2\pi n_o}{\Delta t} \qquad (3\text{-}53)$$

$$\omega_{s_+} = \frac{2\pi(n_o+1)}{\Delta t}$$

A computer program was written to make the final determination of the correct set of θ, β and ω_s. The procedure involved a double loop which tested the six possible combinations of the ω_s's and (β, θ)'s in equation (3-35) or (3-36) to predict the times and voltages of the maxima and minima. For each of the three possible ω_s's both (θ_1, β_1) and (θ_2, β_2) were tested. The procedure was very sensitive in that the five incorrect possibilities had obvious phase shifts from the observed maxima-minima during precession whereas the one correct combination predicted the maxima-minima times to within the measurement error. The results had the pair (β_1, θ_1) with $\omega_s = \omega_{s_+}$ and the pair (β_2, θ_2) had $\omega_s = \omega_{s_o}$.

In order to specify the attitude of the payload with respect to $\vec{B}$ one needs to determine θ, the coning half-angle, β, the angle between $\vec{L}$ and $\vec{B}$, ϕ, the Euler precession angle and ψ, the Euler spin angle.

ϕ is found from the primary nodes in the envelope curves. The time between them gives τ_p, the precession period. ϕ is found using (3-47). θ and β are found by fitting equations (3-46) for a and b and then simultaneously solving the first two equations of (3-34) for pairs of (θ, β). The choice of which pair of (θ, β) and which ω_s to use is then determined by testing the possible cases to minimize the phase and amplitude errors between results from equations (3-35) or (3-36) and the measured values.

Tables V and VI give the frequency-period results and the angular results respectively.

Table V

Vehicle	Tϕ (first node)	TP (Precession period)	TS (spin period)
18:63	0604:34.38	131.5 sec	1.93976sec
18:64	0409:38.516	185.751	1.05540
18:65	0306:26.245	199.104	1.06209

Table VI

Vehicle	ϕ_o	ψ_o	θ	β	average angle between z'' and $-\vec{B}$	θ, β uncertainty
18:63	$\pi/2$	0	70.2°	205.6°	72°	± 6°
18:64	$\pi/2$	π	20.50	203.4	31°	± 1°
18:65	$\pi/2$	π	9.023°	193.6°	16°	± 2°

APPENDIX I

Evaluation of Euler Angles for Despinning Symmetric Payload

Vehicles 18:64 UE and 18:65 UE carried experiments which required the deployment of long booms. After the yo-yo despin the motors which deployed these booms were switched on. Deployment time was about 100 sec. The booms extended radially, in opposite directions, from the spin axis. Their contribution to the transverse moment of inertia, I_T, was negligible, and the vehicle was assumed to remain axially symmetric. The effect upon the axial moment of inertia, I_A, was significant and resulted in further decreasing the vehicle-spin rate. To make complete use of data from the boom experiments and other experiments during the deployment it was necessary to determine the Euler angles for this time period.

The total time derivative of angular momentum, $\vec{L}$, with respect to inertial coordinates for a varying moment of inertia, $\overleftrightarrow{I}$, and a torque, $\vec{N}$, is given by[3]

$$\vec{N} = \frac{d\vec{L}}{dt} = \overleftrightarrow{I} \cdot \dot{\vec{\omega}} + [\dot{\overleftrightarrow{I}}] \cdot \vec{\omega} + \vec{\omega} \times \vec{L} \tag{A-1}$$

where for a symmetrical payload changing only the axial moment of inertia,

$$\overleftrightarrow{I} = \begin{bmatrix} \hat{i}''\,\hat{i}''\, I_T & 0 & 0 \\ 0 & \hat{j}''\,\hat{j}\, I_T & 0 \\ 0 & 0 & \hat{k}''\,\hat{k}''\, I_A \end{bmatrix}$$

$$[\dot{\overleftrightarrow{I}}] = \begin{bmatrix} 0 & 0 & 0 \\ 0 & 0 & 0 \\ 0 & 0 & \hat{k}''\hat{k}''\dot{I}_A \end{bmatrix}$$

We assume the external torque, $\vec{N} = 0$. The component equations analogous to (3-4) are

$$I_T\dot{\omega}_{x''} + \omega_{y''}I_A\omega_{z''} - \omega_{z''}I_T\omega_{y''} = 0$$

$$I_T\dot{\omega}_{y''} + \omega_{z''}I_T\omega_{x''} - \omega_{x''}I_A\omega_{z''} = 0 \qquad \text{(A-2)}$$

$$I_A\dot{\omega}_{z''} + \dot{I}_A\omega_{z''} + \omega_{x''}I_T\omega_{y''} - \omega_{y''}I_T\omega_{x''} = 0$$

From the last of (A-2) we have

$$I_A\dot{\omega}_{z''} + \dot{I}_A\omega_{z''} = 0 \; ; \quad I_A\omega_{z''} = \text{constant} = a \; . \qquad \text{(A-3)}$$

The magnitude of the total angular momentum, $|\vec{L}|$, is a constant. Because the component of $\vec{L}$ along z'' is constant the Euler angle θ is defined by

$$\sin\theta = \frac{I_A\omega_{z''}}{|\vec{L}|} = \text{constant} \qquad \text{(A-4)}$$

Hence, for our case, θ , the coning angle is constant during the long boom deploy despin.

The first two equations of (A-2) can be manipulated as in (3-7) to (3-9) to give.

$$\omega_{x''}^2 + \omega_{y''}^2 = \text{constant} \equiv \omega_T^2 \tag{A-5}$$

However because $\omega_{z''}$ changes the angular velocity vector doesn't have constant magnitude and the angle ε increases as $\omega_{z''}$ decreases.

$$\tan\theta = \frac{I_T\omega_T}{I_A\omega_{z''}} = \frac{I_T\omega_T}{a} \tag{A-6}$$

$$\tan\varepsilon = \frac{\omega_T}{\omega_{z''}}$$

Using equations (3-17), (3-19) and(A-5) we have $\dot{\phi} = \text{constant} \equiv \omega_p$, and

$$\omega_{z''}(t) = \dot{\psi}(t)+\dot{\phi}\cos\theta \ . \tag{A-7}$$

We define

$$\omega_o \equiv \dot{\phi}\cos\theta = \text{constant} \ . \tag{A-8}$$

then using (A-7), (A-8) and (A-3)

$$\dot{\psi}(t) = \omega_{z''}(t) - \omega_o = \frac{a}{I_A(t)} - \omega_o \ . \tag{A-9}$$

$\dot{\phi}$, ϕ and θ can be determined from the rigid body portion of the flight.

By choosing an appropriate model for $I_A(t)$ we can integrate (A-9), and compute the remaining Euler angle ψ.

The axial moment of inertia can be made from a constant component, A, plus a contribution due to the deploying booms, $I_B(t)$. If the booms deploy at a constant speed $I_{Boom}(t)$ will have quadratic time dependence.

(A-10)
$$I_B(t) = B(t-t_D)^2$$

$$I_A(t) = A+B(t-t_D)^2$$

where t_D is the time the booms begin deploying. We know that the value of A is 2.196 kg-m^2. Using (A-10) we can integrate (A-9) from t_1 to t_2.

(A-11)
$$\psi(t_2)-\psi(t_1) = a\int_{t_1}^{t_2} \frac{dt}{[A+B(t-t_D)^2]} - \omega_o(t_2-t_1)$$

$$\psi(t_2)-\psi(t_1) = \frac{a}{\sqrt{AB}}\left[\tan^{-1}\frac{(t_2-t_D)\sqrt{AB}}{A} - \tan^{-1}\frac{(t_1-t_D)\sqrt{AB}}{A}\right] - \omega_o(t_2-t_1)$$

We drop the suffix on t_1 and let $t_2 = t_f$, the time the long booms complete deployment.

$$\psi(t) = \frac{a}{\sqrt{AB}}\tan^{-1}\left[\frac{(t-t_D)\sqrt{AB}}{A}\right] - \omega_o t + \psi_o$$

(A-12)

where $\psi_o \equiv \psi(t_f) - \psi_f + \omega_o t_f$

and $\psi_f \equiv \frac{a}{\sqrt{AB}}\tan^{-1}\left[\frac{(t_f-t_D)\sqrt{AB}}{A}\right]$

Actually the argument of the inverse tangent is related to the boom moment of inertia

$$\text{(A-13)} \qquad \text{ARG} = \sqrt{\frac{(t-t_D)^2 B}{A}} = \sqrt{\frac{I_B(t)}{A}}$$

We can determine $\psi(t_f)$ by using (3-25) which is appropriate for the part of the flight where I_A is constant.

$$\text{(A-14)} \qquad \psi(t_f) = \omega_S(t_f - t_o) + \pi$$

Two more constants, a and B , remain to be evaluated to determine (A-12). From magnetometer data we can measure the observed spin period, $\tau_S(t)$. It depends upon ϕ and θ as well as ψ because during most of the flight $\dot{\psi}$ is constant whereas τ_S deviates as the vehicle approaches its nearest position to the magnetic field. However for times $> 0.05\tau_p$ from one of these magnetometer envelope nodes we can write

$$\text{(A-15)} \qquad \tau_S(t)/2\pi \doteq \frac{1}{\dot{\psi}}$$

then using (A-9) we have

$$\text{(A-16)} \qquad \tau_S(t) \doteq \frac{2\pi}{a - \omega_o I_A(t)}$$

Using (A-10) and making an expansion for $a >> \omega_o A$, one obtains

$$\text{(A-17)} \qquad \tau_S(t) = \frac{2\pi A}{a-\omega_o A} + \frac{2\pi B(t-t_D)^2}{(a-\omega_o A)} \left[1 + \frac{\omega_o A}{(a-\omega_o A)}\right]$$

Equation (A-17) is now in a form which can be least squares fitted by

$$\tau_S(t) = C_1 + C_2(t-t_D)^2 \quad . \tag{A-18}$$

Using the values of C_1 and C_2 determined by the fitting we have

$$a = \frac{2\pi A}{C_1} + \omega_o A \tag{A-19}$$

$$B = \frac{C_2(a-\omega_o A)}{2\pi\left[\frac{\omega_o A}{(a-\omega_o A)} + 1\right]} \tag{A-20}$$

The constant B is proportional to the rate at which the booms deploy. We found that the spin rate indicated that they deployed at two rates, a slow initial rate and then at a higher rate until they were completely deployed. Consequently equation (A-12) had to be used twice with separate values of a and B .

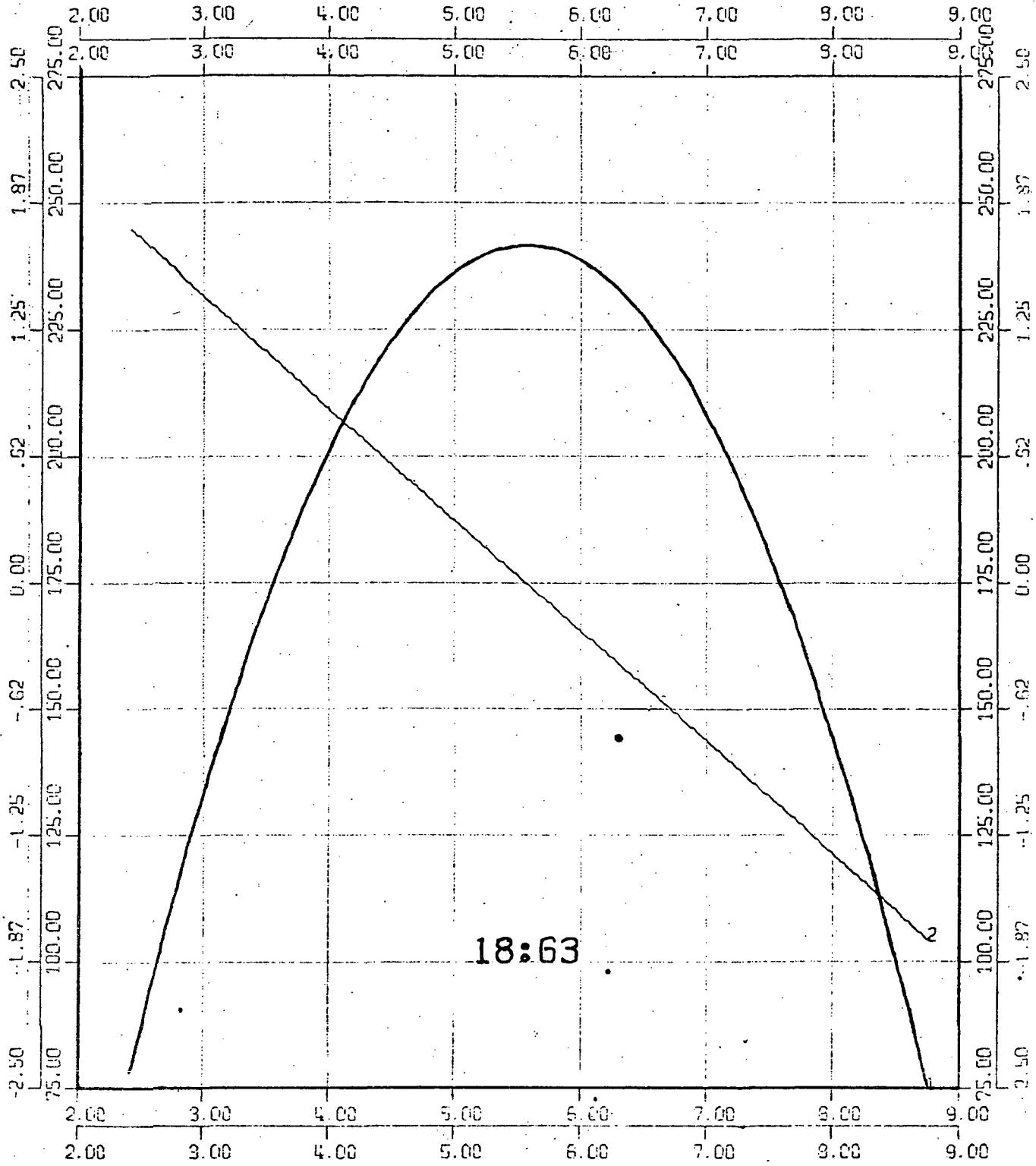

ALTITUDE AND VELOCITY VS. UNIVERSAL TIME

FIGURE 1

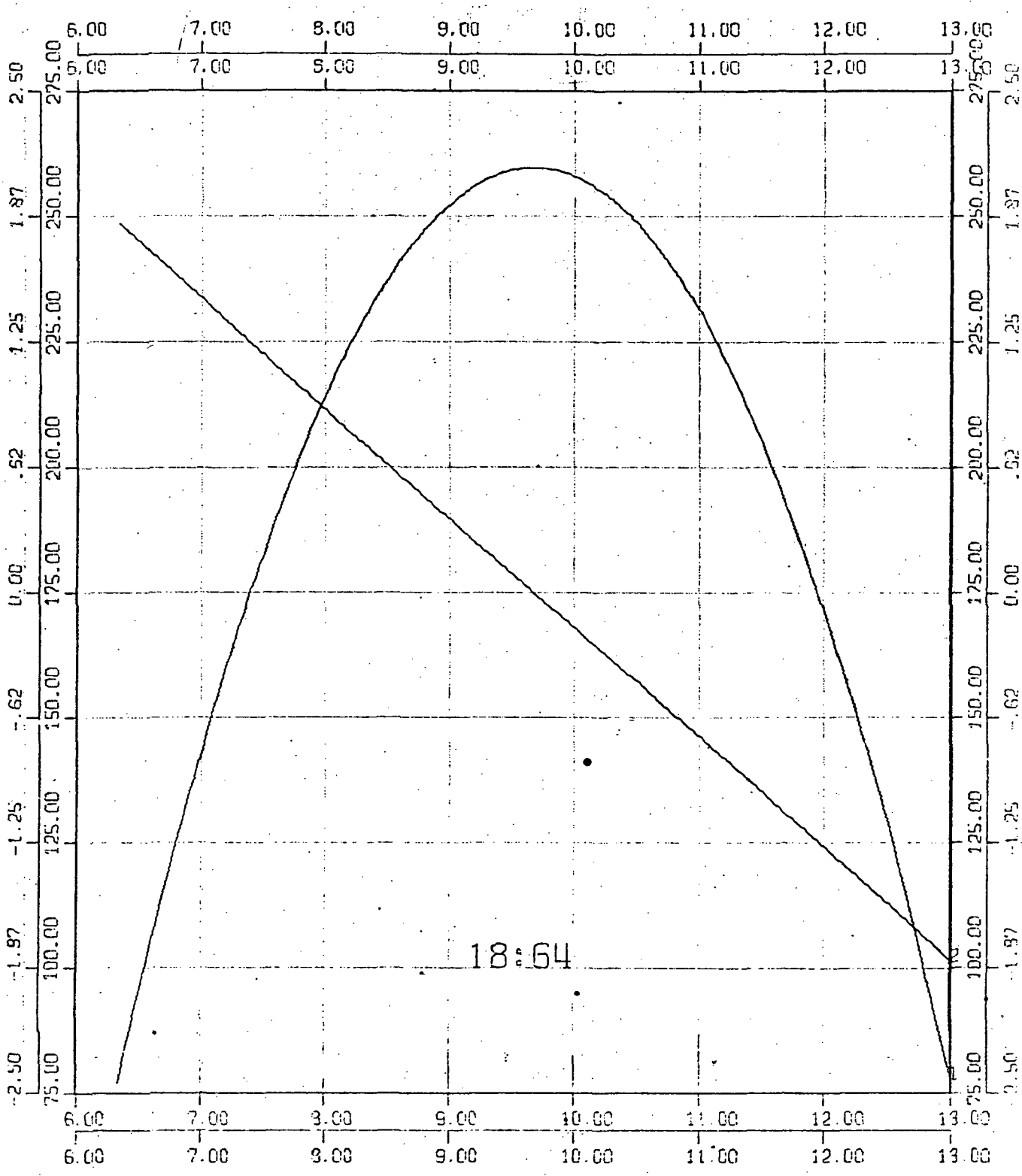

ALTITUDE AND VELOCITY VS. UNIVERSAL TIME

FIGURE 2

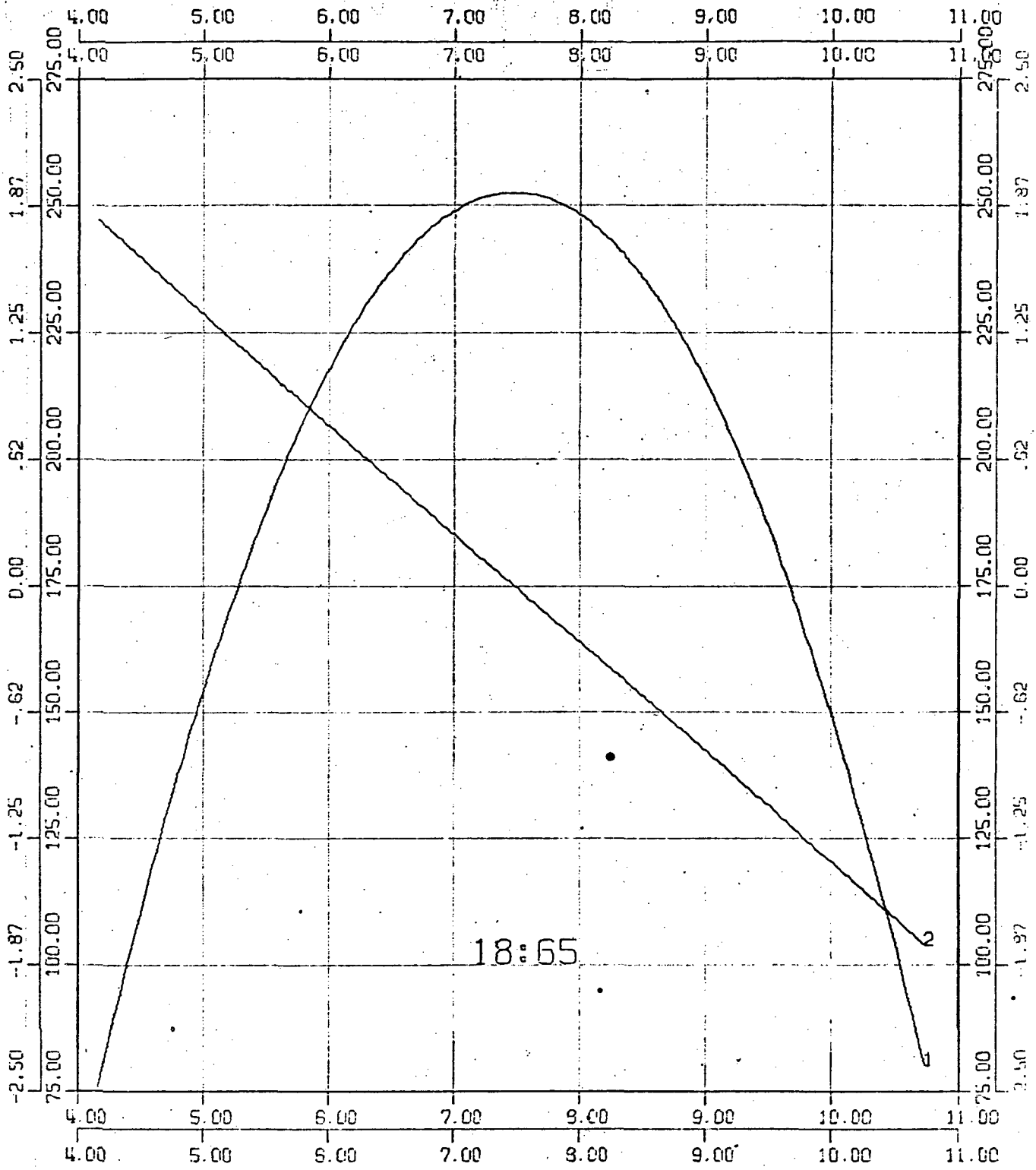

ALTITUDE AND VELOCITY VS. UNIVERSAL TIME

FIGURE 3

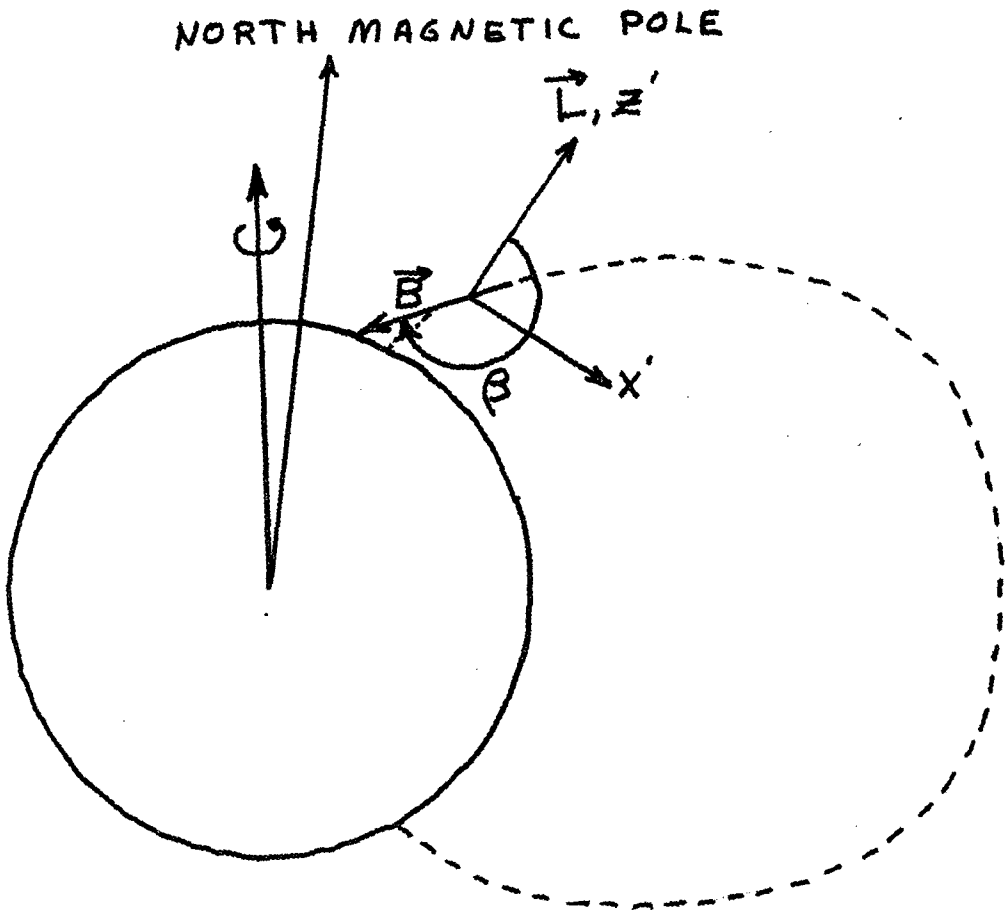

TYPICAL ORIENTAION OF PRIMED COORDINATE SYSTEM

FIGURE 4

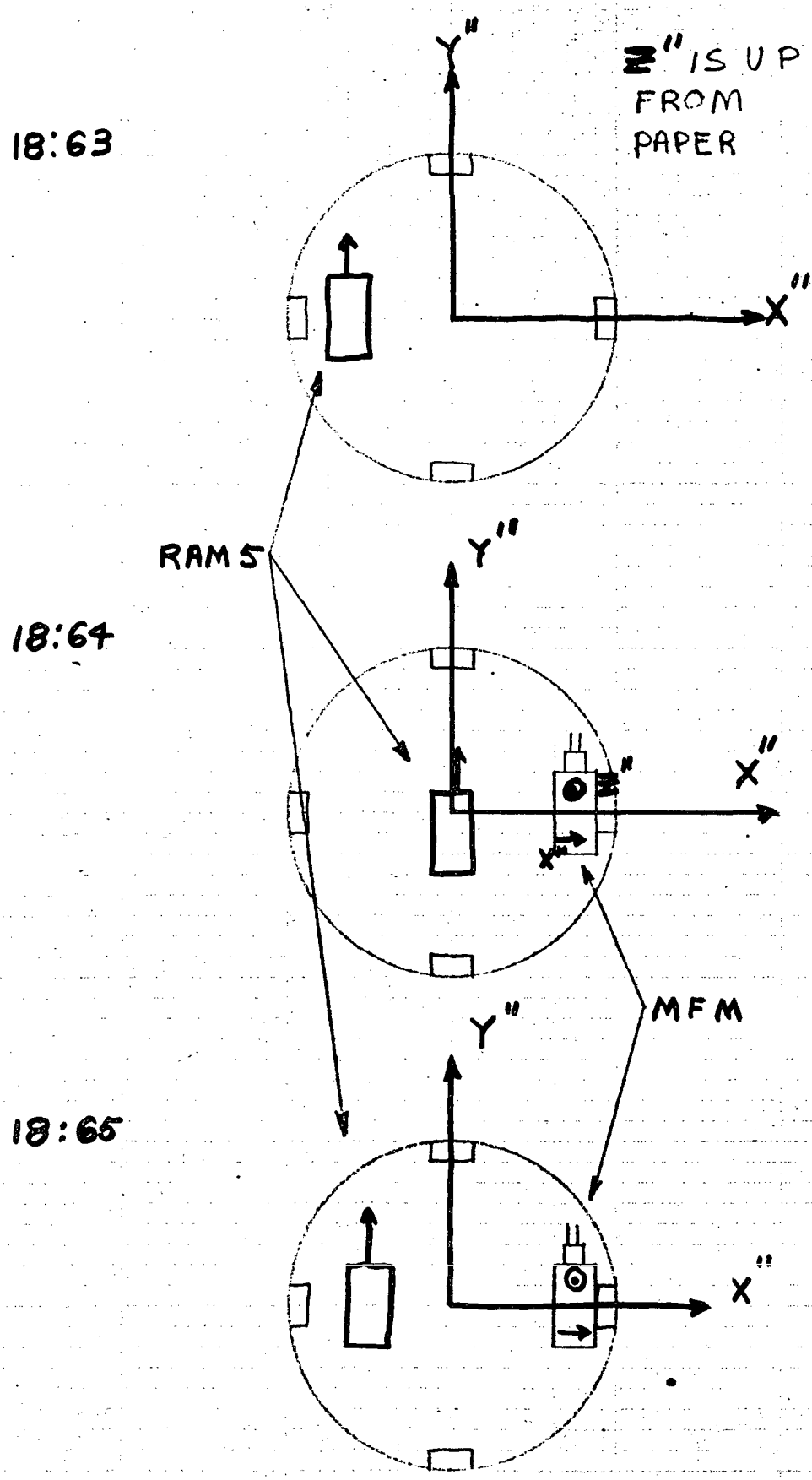

MAGNETOMETER POSITIONS

FIGURE 5

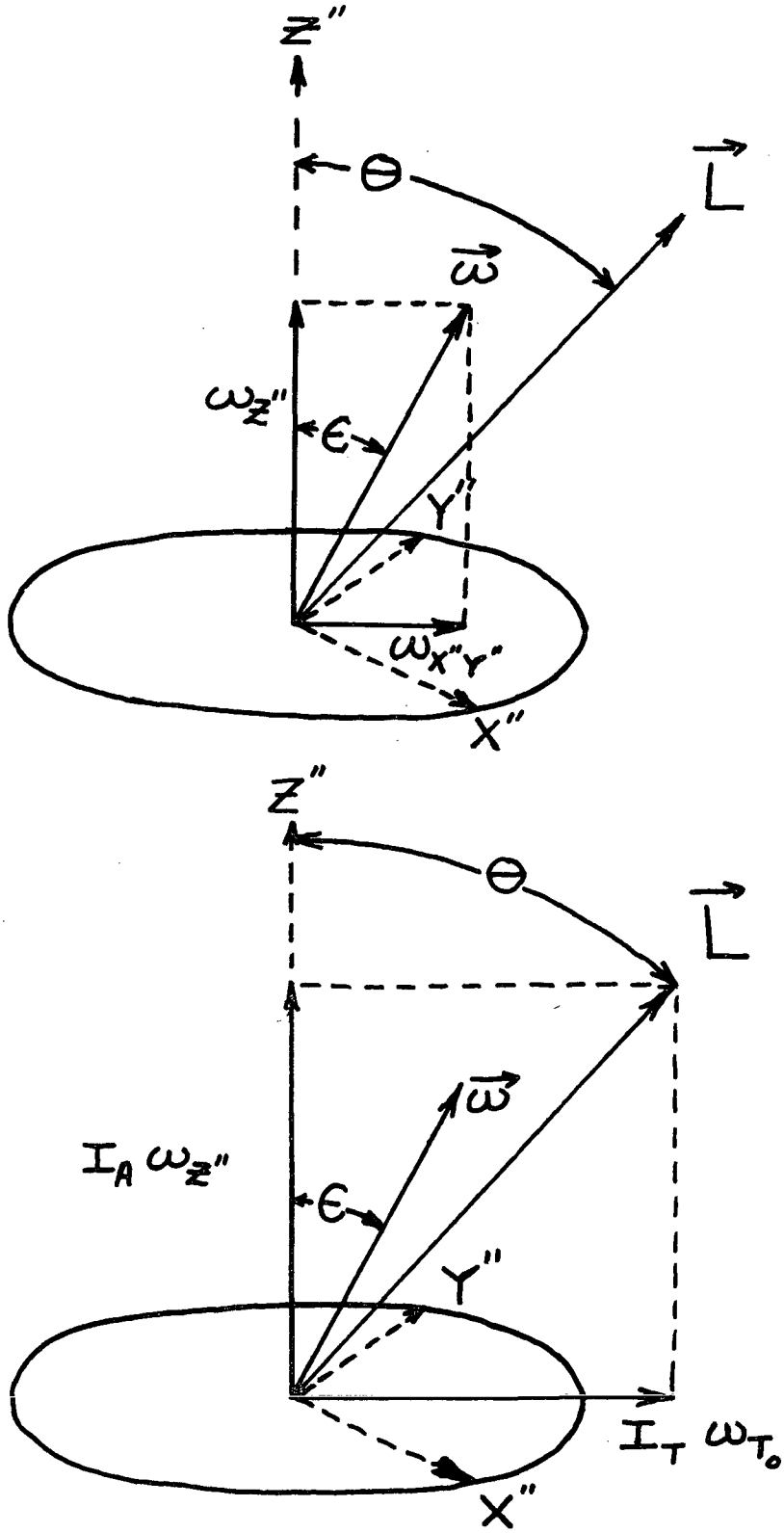

ATTITUDE DYNAMICS COORDINATES

FIGURE 6

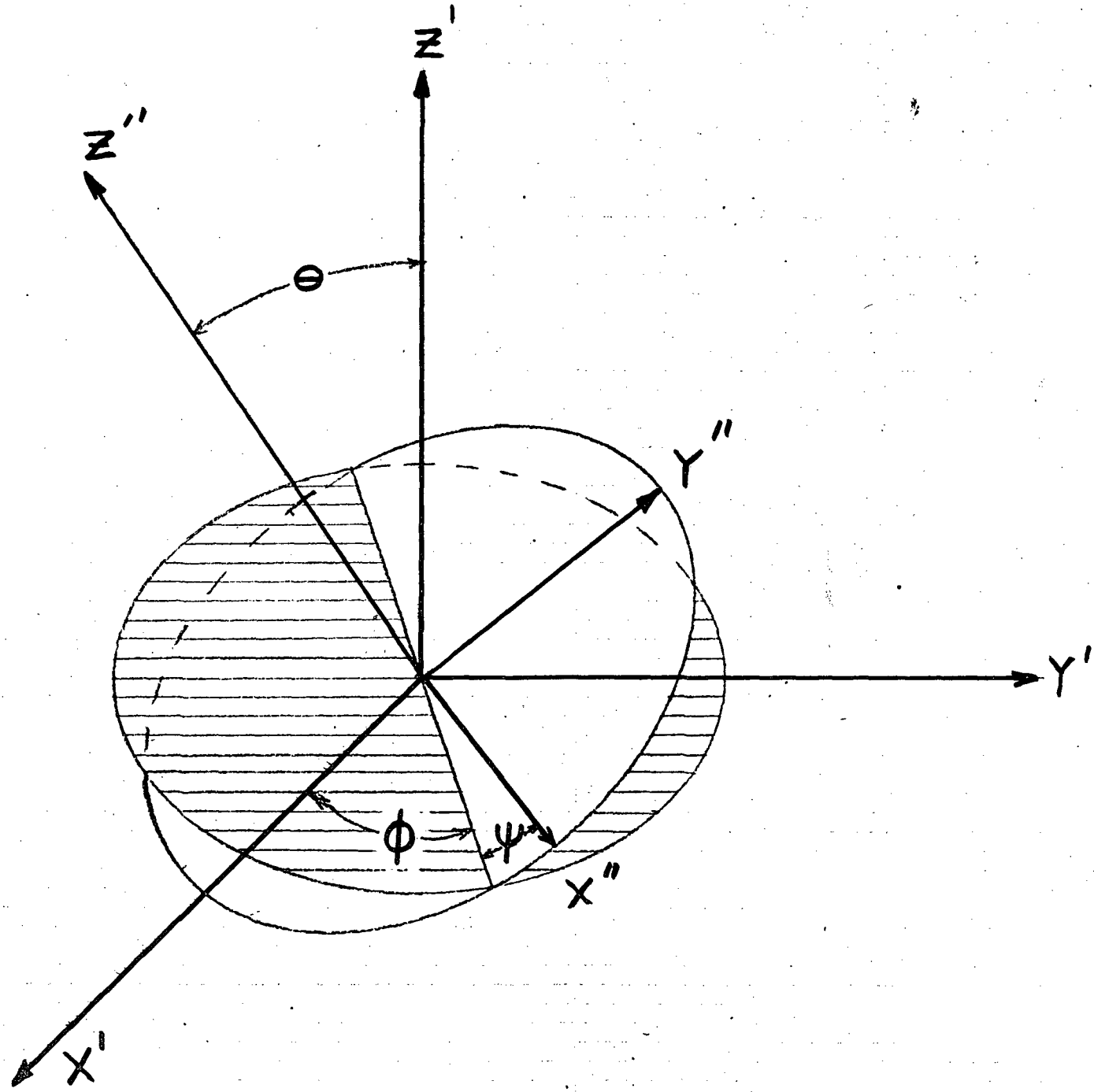

FIGURE 7

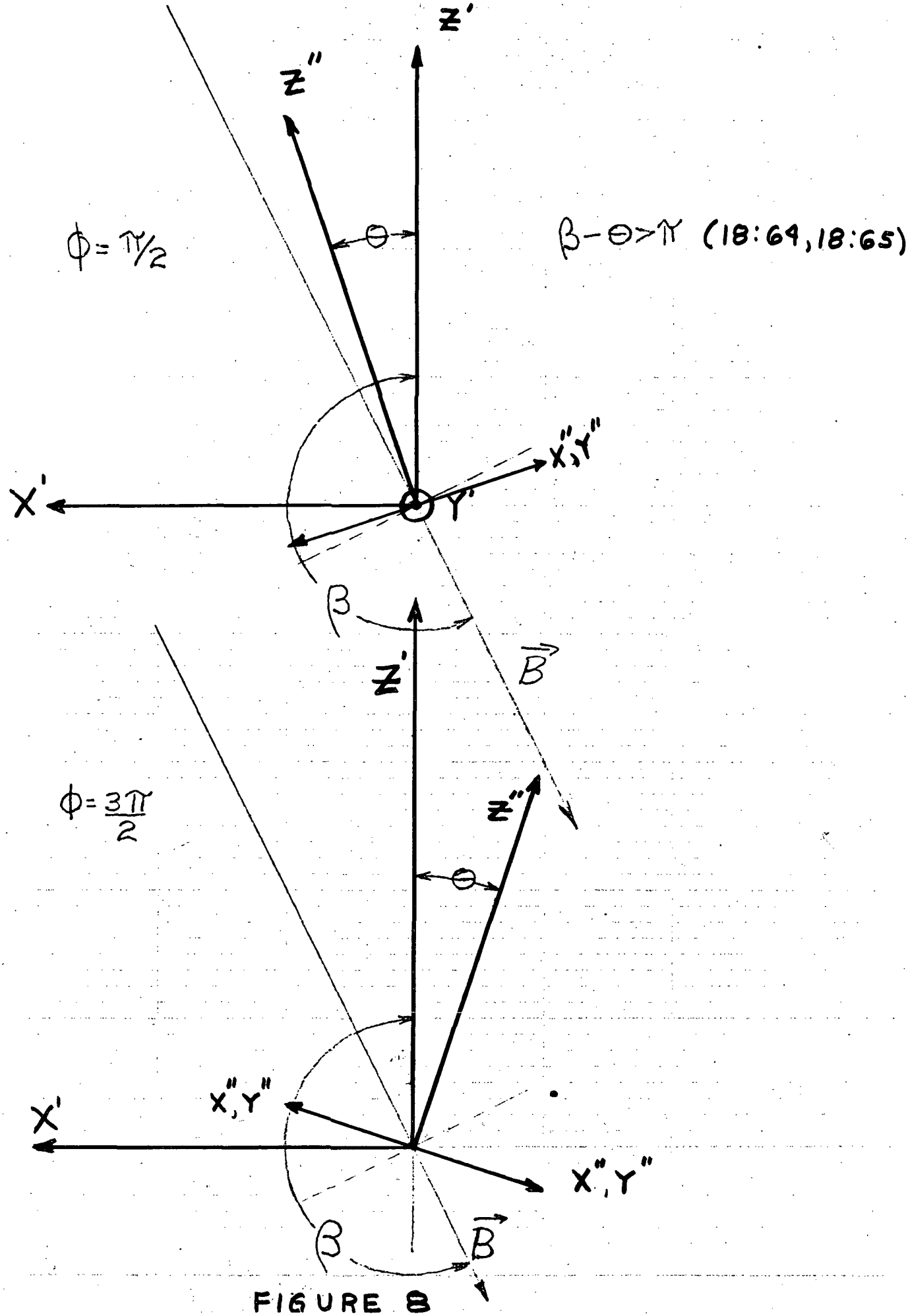

FIGURE 8

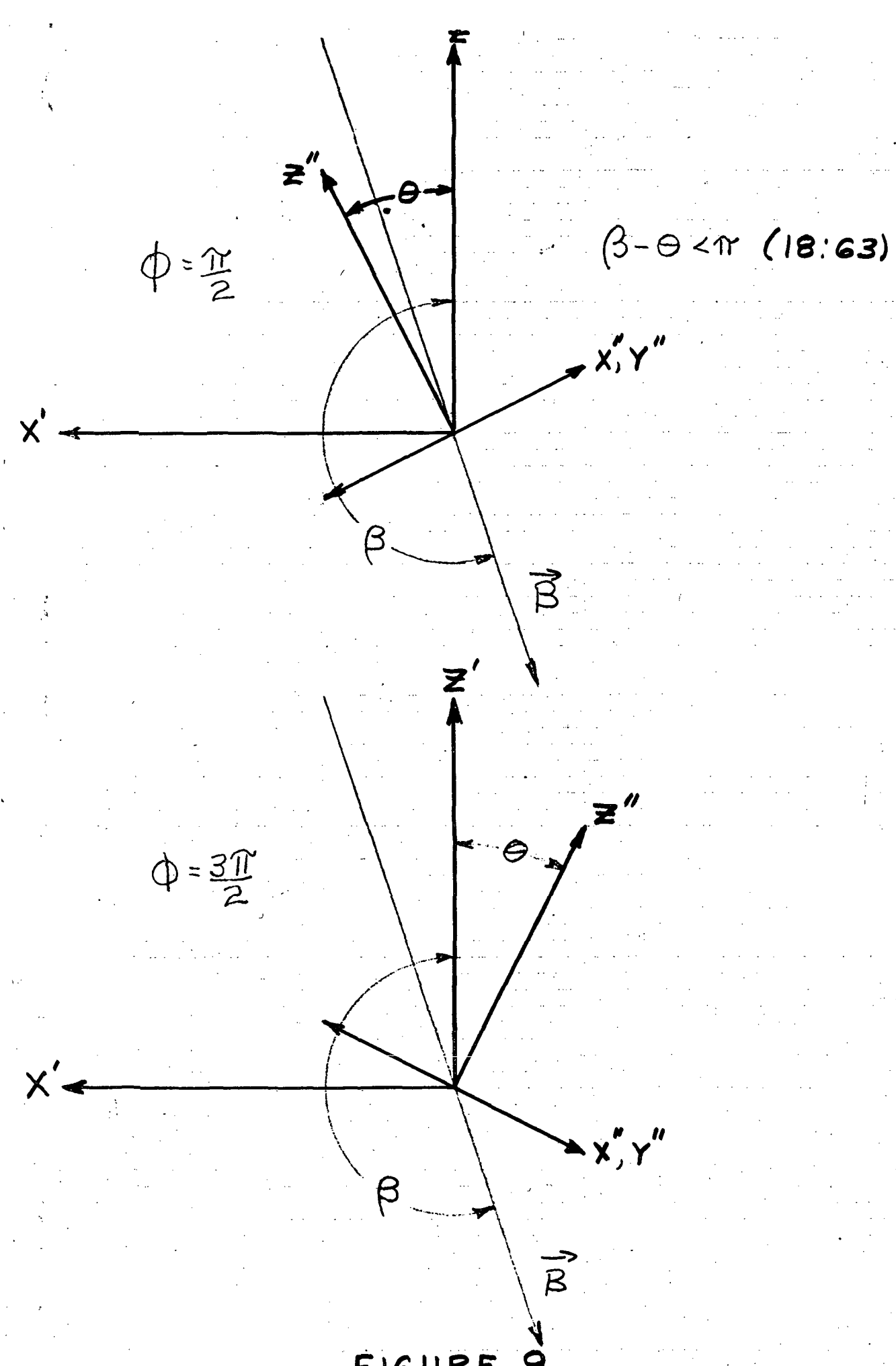

FIGURE 9

NORMAL ENVELOPE

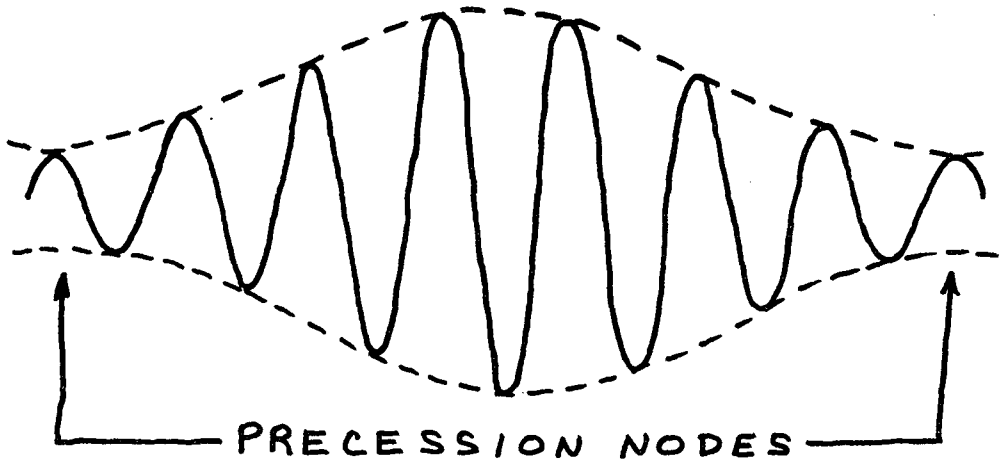

18:63 TYPE ENVELOPE

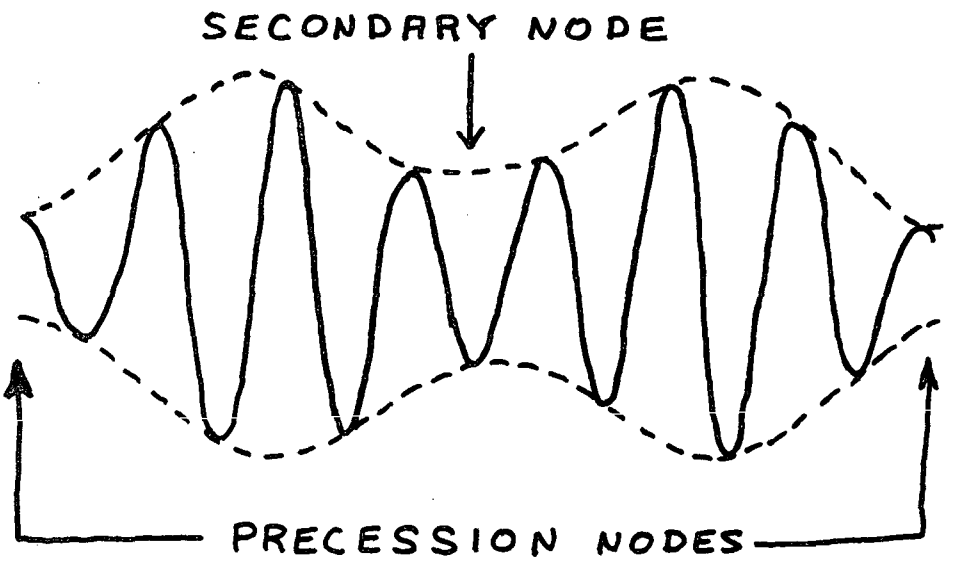

LATERAL MAGNETOMETER OUTPUTS

FIGURE 10

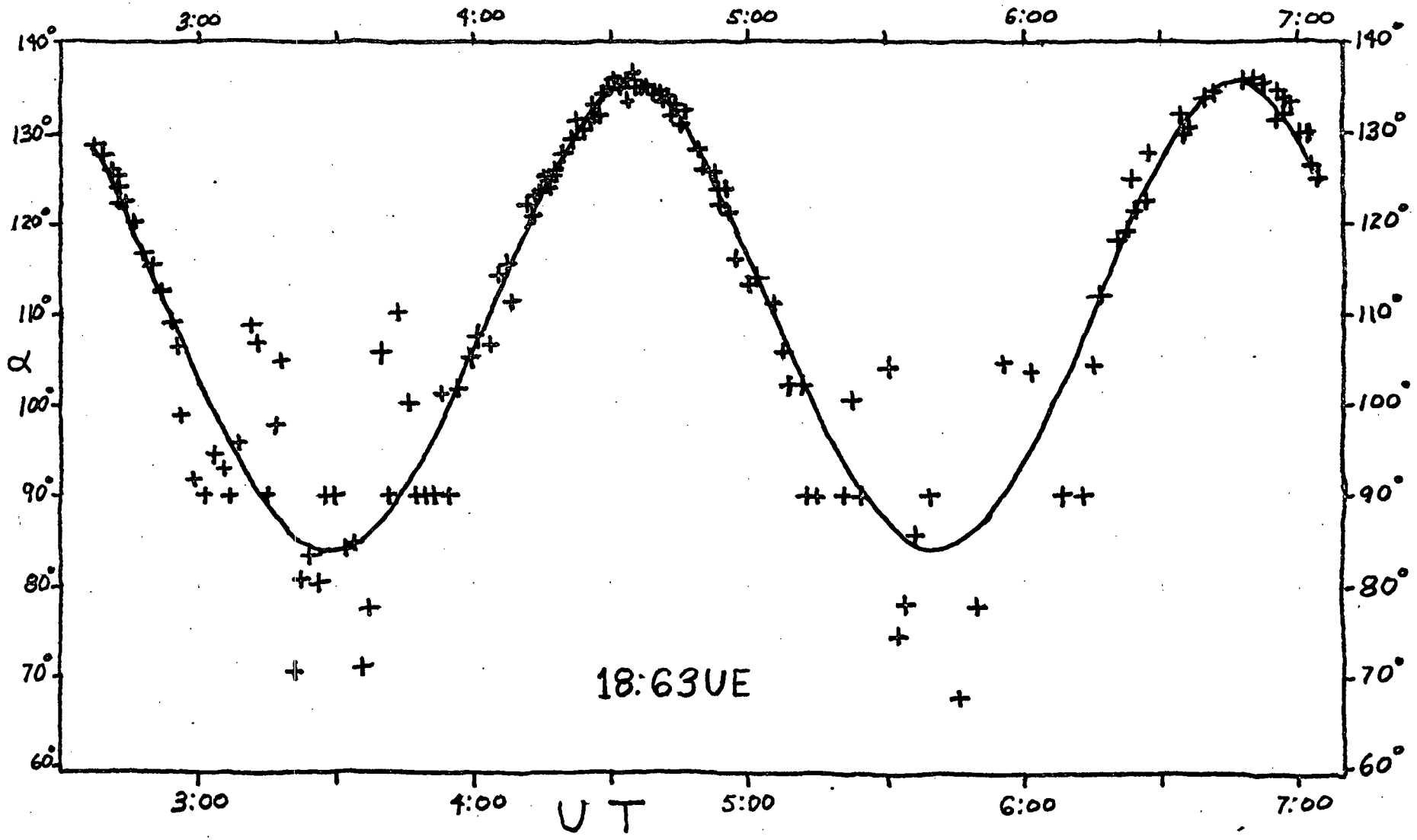

PLOT OF MEASURED AND COMPUTED VALUES OF α-ANGLE BETWEEN SPIN AXIS AND MAGNETIC FIELD.

FIGURE 11